Environmental Science & Technology

pubs.acs.org/est

Article

Characterizing the Opportunity Space for Sustainable Hydrothermal Valorization of Wet Organic Wastes

Jianan Feng, Yalin Li, Timothy J. Strathmann, and Jeremy S. Guest*

Cite This: *Environ. Sci. Technol.* 2024, 58, 2528−2541

Read Online

ACCESS | Metrics & More | Article Recommendations | Supporting Information

ABSTRACT: Resource recovery from wet organic wastes can support circular economies by creating financial incentives to produce renewable energy and return nutrients to agriculture. In this study, we characterize the potential for hydrothermal liquefaction (HTL)-based resource recovery systems to advance the economic and environmental sustainability of wastewater sludge, FOG (fats, oils, and grease), food waste, green waste, and animal manure management through the production of liquid biofuels (naphtha, diesel), fertilizers (struvite, ammonium sulfate), and power (heat, electricity). From the waste management perspective, median costs range from −193 $·tonne^{-1} (FOG) to 251 $·tonne^{-1} (green waste), and median carbon intensities range from 367 kg CO_2 eq·tonne^{-1} (wastewater sludge) to 769 kg CO_2 eq·tonne^{-1} (green waste). From the fuel production perspective, the minimum selling price of renewable diesel blendstocks are within the commercial diesel price range (2.37 to 5.81 $·gal^{-1}) and have a lower carbon intensity than petroleum diesel (101 kg CO_2 eq·MMBTU^{-1}). Finally, through uncertainty analysis and Monte Carlo filtering, we set specific targets (i.e., achieve wastewater sludge-to-biocrude yield >0.440) for the future development of hydrothermal waste management system components. Overall, our work demonstrates the potential of HTL-based resource recovery systems to reduce the costs and carbon intensity of resource-rich organic wastes.

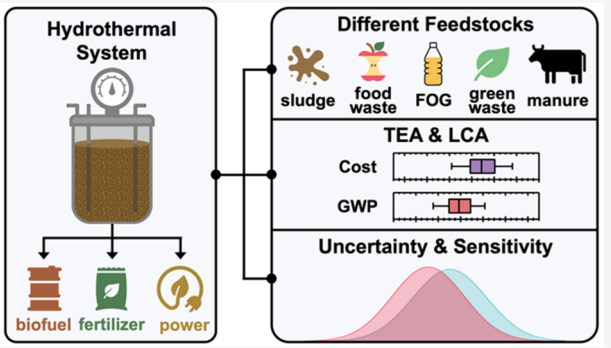

KEYWORDS: *circular bioeconomy, catalytic hydrothermal gasification (CHG), resource recovery, techno-economic analysis (TEA), life cycle assessment (LCA), greenhouse gas (GHG), quantitative sustainable design (QSD)*

INTRODUCTION

More than 100 million tonnes (i.e., metric tons) of wet organic wastes, including wastewater sludge, FOG (fats, oils, and grease), food waste, green waste (waste from gardening and landscaping), and animal manure, were produced in the United States in 2017.[1,2] These wastes represent a very real challenge for waste management due to their high production rate and the inefficiency of conventional management methods. Currently, the majority of these wastes are sent to landfills, leading to significant amounts of greenhouse gas (GHG) emissions. For example, food waste—the single largest component of municipal solid waste sent to landfills—represents more than 15% of total U.S. human-caused methane emissions,[2] and nutrients in these wastes can cause additional environmental consequences (e.g., via leachate and runoff[3]). Other common resource recovery methods, such as incineration and anaerobic digestion with land application, can also lead to unwanted environmental consequences including fugitive NO_x emissions during incineration[4] or the release of antibiotic resistant bacteria,[5,6] heavy metals,[7] or emerging contaminants like per- and polyfluorinated substances (PFAS)[8] from the land application of biosolids. Further, these management methods are costly (40 to 880 $·tonne^{-1}[9,10]) and often underutilize the resource potential embedded in organic wastes. Alternatively, these waste streams have the potential to serve as feedstocks for biofuels and bioproducts and support broader efforts to decarbonize communities.[1]

One promising technology for wet organic waste valorization is hydrothermal liquefaction (HTL), which converts wet organic wastes (50 to 90% moisture) under subcritical to supercritical temperatures (250 to 450 °C) into four product phases: biocrude oil, aqueous phase, hydrochar, and the CO_2-dominant gas phase.[11−13] Among these products, biocrude has high organic content and can be refined through hydrotreating and hydrocracking to produce drop-in liquid biofuels (e.g., naphtha, diesel).[14] The aqueous phase can also have organic compounds, with compositions dependent on the feedstock and reaction conditions. With regard to nutrients, feedstock nitrogen is distributed between the biocrude and aqueous

Received: September 7, 2023
Revised: November 18, 2023
Accepted: December 26, 2023
Published: January 24, 2024

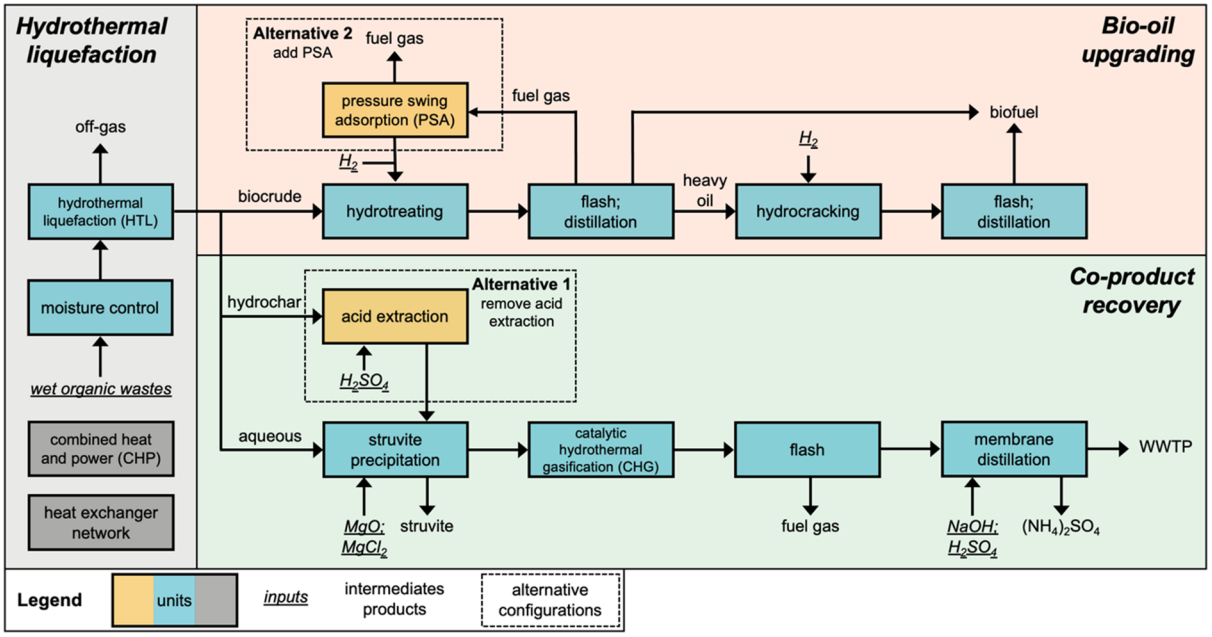

Figure 1. Simplified flowchart of the hydrothermal waste management system. The system was separated into three parts: hydrothermal liquefaction (HTL) and supporting units (left, gray shaded region), bio-oil upgrading (upper right, orange shaded region), and coproduct valorization (lower right, green shaded region). Inside-battery limit and outside-battery limit units are shown in blue and gray blocks, respectively. Units in yellow blocks relate to decision variables in alternative design scenarios. Specifically, an acid extraction unit was included in the baseline design but was excluded in one scenario (Alternative 1) to consider trade-offs stemming from phosphorus recovery, and a pressure swing adsorption unit was not included in the baseline design but was added in another scenario (Alternative 2) to explore the impacts of recycling hydrogen gas. WWTP stands for wastewater treatment plant. Some processes and streams were not included for figure clarity; full-scale system configurations are available online.[46]

phases, whereas feedstock phosphorus is distributed between the hydrochar and aqueous phases.[14] Nutrients embedded in the aqueous and hydrochar product phases can be recovered by further processing (e.g., precipitation of P- and N-containing struvite; gasification of aqueous organic nitrogen and electrochemical stripping of the resulting ammonia).[15−17] By selling these products, hydrothermal waste management systems have the potential to drive down net waste management costs. In addition, HTL may help address environmental concerns related to emerging contaminants (e.g., it has been reported HTL can destroy persistent organic pollutants like PFAS which can accumulate in waste organic feedstocks[18,19]).

HTL has been applied to multiple organic wastes including wastewater sludge,[20−22] FOG,[23,24] food waste,[25−27] animal manure,[27−29] green waste,[30] and their mixtures.[22,31,32] These feedstocks have different biochemical (carbohydrate, protein, lipid) compositions and macrostructures, leading to variabilities in product yields and characteristics (e.g., the energy content of biocrude). For example, FOG (which are nearly 100% lipids) has a high biocrude yield of more than 80% but very low nutrient recovery potential,[23] while gases and hydrochar have been reported to be the main products from carbohydrate-rich feedstocks such as green waste.[30] To better understand the full-scale implications of HTL for waste valorization, several models have been developed to predict HTL performance[33−36] and techno-economic analysis (TEA) and life cycle assessment (LCA) studies have examined the economic viability and environmental impacts of hydrothermal waste management systems. Previously, LCAs on cultivated feedstocks such as microalgae have demonstrated the environmental benefits of HTL (e.g., a carbon intensity of −1.2 to 40.1 kg CO_2 eq·MMBTU^{-1},[37−39] compared to the 101 kg CO_2 eq·MMBTU^{-1} reported for fossil fuels[39]), but TEAs have demonstrated high feedstock costs (e.g., 331 to 779 $·tonne^{-1} for microalgae[15,40]) can significantly undermine the financial viability of the integrated feedstock-to-biofuel system (e.g., achieving a minimum fuel selling price [MFSP] of 4.49 to 12.1 $·gal^{-1},[37,38,40,41] compared to the average diesel price of 3.13 $·gal^{-1} from 2018 to 2022[42]). Alternatively, high-organic-content waste streams are generated as products of societal metabolism and generally incur costs to manage. Thus, entities operating HTL-based treatment trains could potentially acquire low-cost (or even negative cost; e.g., a tipping fee can be charged for managing the waste[43]) feedstocks, thereby creating an opportunity for a financially viable and low-environmental impact alternative for waste management through resource recovery and processing.[44]

The objectives of this work were (i) to characterize the economic and environmental sustainability of HTL-based treatment trains for the management and valorization of wet organic wastes and (ii) to set research and development targets for key technological parameters (e.g., minimum biocrude yield) for HTL-based resource recovery systems to outcompete conventional approaches to waste management. To this end, we leveraged two open-source modeling platforms—QSDsan[45,46] and BioSTEAM[47,48]—for the design, simulation, TEA, and LCA of hydrothermal waste management systems under uncertainty. We focused our analyses on five representative wet organic wastes identified in the U.S. DOE's waste-to-energy report[1] and U.S. EPA's organic waste management report[2] (wastewater sludge, FOG, food waste, green waste, and animal manure) and benchmarked the performance of a HTL-based resource recovery system against

https://doi.org/10.1021/acs.est.3c07394
Environ. Sci. Technol. 2024, 58, 2528−2541

conventional waste management strategies. We further performed global sensitivity analyses to identify drivers of uncertainty and Monte Carlo filtering to set explicit targets for key technological parameters to achieve financial viability. In addition to these technological parameters, we also evaluated the implications of two decision variables (whether to include phosphorus recovery and/or hydrogen recycling) and two contextual parameters (plant size and internal rate of return) which are critical to the successful deployment of hydrothermal waste management systems. Overall, this study supports the potential of hydrothermal systems and HTL-based resource recovery trains for the management and valorization of wet organic wastes and provides guidance on the prioritization of research and development targets to increase the opportunities for successful technology deployment.

METHODS

System Description. The system modeling, simulation, and analyses were performed in QSDsan and BioSTEAM. Specifically, a hydrothermal waste management system (Figure 1) was designed with a daily capacity of 100 dry tonnes (this value was adjusted in the sensitivity analysis) and simulated over 30 years of operation. The system was designed to receive wet organic wastes and adjust the moisture content to 80% by adding water if necessary for HTL reactions,[49] after which the wet feedstocks were pressurized and heated before being fed into the HTL reactor.[40] The conversion of feedstocks to biocrude oil, an aqueous phase, off-gas and hydrochar was simulated to occur within 15 min at 350 °C and 21 MPa under air headspace, a condition that has been previously reported for HTL-based organic waste conversions.[22,50] Then, the HTL products were passed through knockout drums for gas separation and a solid filter for hydrochar recovery. The biocrude and aqueous phases were then separated through a gravimetric oil/water separator.[40,51] The separated biocrude oil was upgraded through hydrotreating to remove heteroatoms (i.e., non-carbon/-hydrogen elements) using presulfided CoMo/alumina catalyst (cobalt molybdenum on an alumina support)[40] under high-pressure hydrogen.[52] The upgraded bio-oil was then fractionated into fuel gas, naphtha, diesel, and heavy oil based on the boiling points via a simulated series of flash vessels and distillation columns. The heavy oil was further processed by hydrocracking using presulfided Co/Mo catalyst[40] under a hydrogen headspace to break down the large-molecule compounds into naphtha and diesel.[52] Similar to hydrotreating, the hydrocracking products were separated via flash vessels and distillation columns. The compositions of hydrotreating and hydrocracking oil products (Table S6 in the Supporting Information, SI) were based on simulated results following the methodology of Jones et al.[40]

The vented fuel gases from hydrotreating and hydrocracking contained more than 90% v/v H_2 and were sent to a combined heat and power (CHP) unit to meet the system's heating needs; excess energy was used to generate electricity that was sold to the local grid. HTL-produced hydrochar was treated with 0.5 M sulfuric acid at 1 g:10 mL to extract phosphorus. The extractant was mixed with the HTL aqueous phase[14] and was supplemented with $MgCl_2$ for struvite ($NH_4MgPO_4 \cdot 6H_2O$) precipitation. A catalytic hydrothermal gasification (CHG) unit was designed to generate additional value by mineralizing and gasifying the residual dissolved organics in the aqueous phase (typically $g \cdot L^{-1}$ concentrations) to fuel gases with 7.8% Ru/C as the catalyst (i.e., 7.8% w/w ruthenium on a carbon support; ruthenium is an active hydrogenolysis catalyst that is selective for volatile hydrocarbons production[53,54]).[40] The produced fuel gases contained approximately 70% v/v CH_4[40] (Table S6) and were sent to the CHP unit. CHG effluent was then directed to a membrane distillation unit to recover the remaining ammonium (NH_4^+).[55−59] In the feed stream of membrane distillation, pH and temperature were maintained at values >10 and >60 °C, respectively, so $NH_3(g)$ was the dominant species; the separated $NH_3(g)$ was absorbed by a 5% sulfuric acid sweep solution to produce ammonium sulfate ($(NH_4)_2SO_4$). Facilities included a system-wide heat exchanger network (designed through pinch analysis with a minimum approach temperature of 86 °C, consistent with the minimum temperature difference observed in heat exchangers in Jones et al.;[40] Figure S1) to offset part of the system's heating and cooling demand.[60] It should be noted that we used a retroactive method for the system's heating and cooling utilities demand calculation. Specifically, we built our model first without CHP or a heat exchanger network. Then, we added these two units to reduce the system's utilities demand, determining the cost reduction and carbon intensity reduction from utility offsets. A detailed description of the full system (e.g., reactor parameters, unit process conditions) is provided in the Supporting Information (section S2) and all python scripts for the system setup and analyses (described in the following sections) are available online.[46]

Mass and Energy Balance. The biochemical compositions of feedstocks—with the ash-free portion comprised of lipid, protein, and carbohydrate (initially modeled as $C_8H_{16}O$, $C_{16}H_{24}O_5N_4$, and CH_2O, respectively,[61] and varied in the uncertainty analysis)—were used as input parameters for a multiphase component additivity model to predict HTL yields and product characteristics.[34] It should be noted that we simplified the assumed composition of green waste, which can also have a relatively high content (8% to 29%)[62] of degradation-resistance lignin.[63−65] The effect of this assumption is discussed in the Opportunities and Challenges section. Consistent with past work, the coefficients of the model parameters for the aqueous phase were adjusted to fulfill mass balance requirements (as described in Leow et al.;[15] Tables S3 and S4). This model has been validated for wastewater sludge and animal manure in Li et al.[34] and was validated in this study for other organic wastes using data from the literature (Table S5). Additional details can be found in section S3 of SI.

Techno-economic Analysis (TEA) and Life Cycle Assessment (LCA). For TEA, capital cost and operation and maintenance cost (e.g., chemicals, catalysts, labor) calculations were automated using existing algorithms in QSDsan[66] and the results were included in the Supporting Information (section S4). The TEA was performed through discounted cash flow rate of return analysis (with a net present value of 0) with two framings: (i) a *waste management* perspective, such that the waste management price (per dry tonne of waste managed) was calculated assuming produced biofuels and fertilizers can be sold at their market price, and (ii) a *renewable diesel producer* perspective, such that the minimum diesel selling price (MDSP) was calculated assuming waste generators would continue to pay existing market prices for waste management. To reflect the likely financing mechanisms for these two cases, different internal rates of return (IRR; the annual rate of growth an investment is expected to generate) and interest rates (the rate paid on a

https://doi.org/10.1021/acs.est.3c07394
Environ. Sci. Technol. 2024, 58, 2528−2541

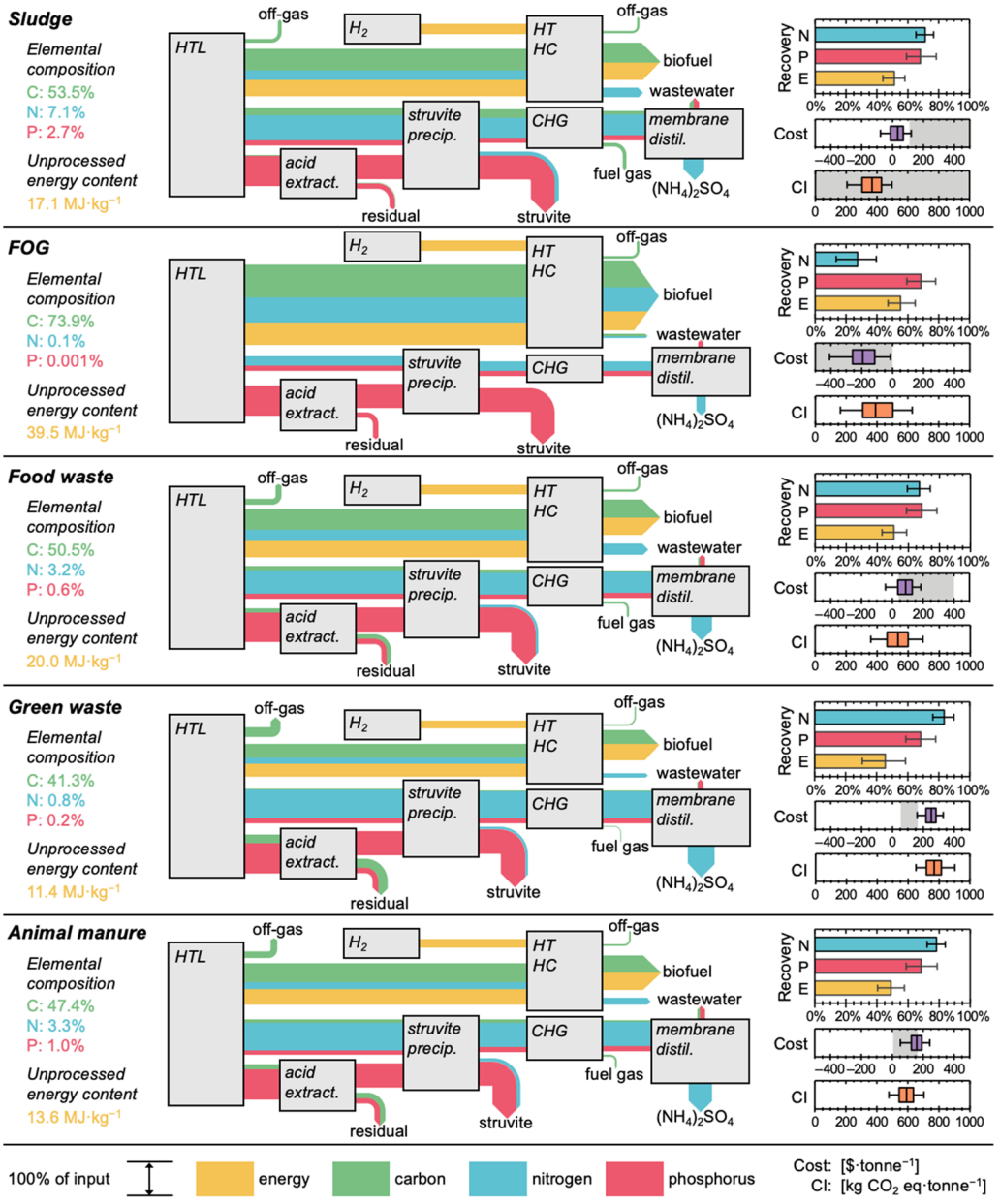

Figure 2. Comparison of carbon (C), nutrient (N, P), and energy (E) recovery rate, waste management costs, and carbon intensity (CI) for hydrothermal liquefaction (HTL)-based waste valorization systems receiving different feedstocks (wastewater sludge, FOG, food waste, green waste, and animal manure). Left panel shows the elemental compositions (as fractions of ash-free dry weight) and unprocessed energy content of each feedstock. In the middle, Sankey diagrams showed average flows of C, N, P, and E through each stage of the treatment train (acid extract.: acid extraction; struvite precip.: struvite precipitation; HT: hydrotreating; HC: hydrocracking; CHG: catalytical hydrothermal gasification; membrane distill.: membrane distillation). All flows were scaled to 100% of initial inputs, as indicated in the figure legend along the bottom. Streams accounting for less than 1% of the elemental mass or energy as well as energy that was consumed internally (i.e., energy associated with carbon in the aqueous phase was consumed in the combined heat and power unit to provide system heating utilities) were not shown for figure clarity. On the right side, bar charts reflected the average N, P, and E recovery ratio with the error bar representing 5th to 95th percentiles. Box plots show the waste management cost and the caron intensity. Whiskers, boxes, and midlines represented 5th/95th, 25th/75th, and 50th percentile values. Gray-shaded areas represent ranges of cost and CI associated with the current waste management methods. The absence of a gray bar means that the related data were not readily available. For wastewater sludge, the gray areas only cover part of the current management cost (110 to 882 $·tonne^{-1}) and CI (−245 to 2200 kg CO_2 eq·tonne^{-1}) for figure readability. All uncertainty results were from 1000 Monte Carlo simulations.

loan) were assumed. In the case of waste management, both IRR and interest rate had a baseline value of 3% given that utilities may be eligible for low interest loans (e.g., 0 to 5% through the State Revolving Loan Fund in the United States[67,68]) and it is appropriate to use the same value for IRR and interest rate when developing planning level costs for utilities.[67] From the renewable diesel producer perspective, capital investment was assumed to come from venture capital with an expected IRR of 10% and an interest rate of 8%, which are consistent with Snowden-Swan et al.[22] All costs were converted to 2020 U.S. dollars using Gross Domestic Product chain-type price index and the Chemical Engineering Plant Cost Index (also consistent with Snowden-Swan et al.[22]). A

https://doi.org/10.1021/acs.est.3c07394
Environ. Sci. Technol. 2024, 58, 2528−2541

complete list of assumptions for the cash flow rate of return analysis can be found in Table S9.

For LCA, life cycle inventory data were acquired from the Ecoinvent v3.8 database[69] (Table S10) and the U.S. EPA's Tool for the Reduction and Assessment of Chemicals and Other Environmental Impacts (TRACI)[70] was used for life cycle impact assessment. From the *waste management* perspective, LCA results were normalized per dry tonne of waste managed, which considers credits (i.e., offsets) from the generated biofuels and fertilizers. From the *renewable diesel producer* perspective, the LCA results were normalized per MMBTU (million British thermal units) of diesel produced, including impact offsets by avoiding traditional waste management strategies. LCA findings in the results and discussion center on carbon intensity (i.e., global warming potential, GWP), but other TRACI indicators are also reported in SI (Table S14).

Uncertainty, Sensitivity, and Scenario Analyses. For uncertainty analysis, we performed Monte Carlo simulations with Latin hypercube sampling (N = 1000) for 78 decision variables, technological parameters, and contextual parameters[71] in addition to life cycle inventory data and characterization factors (a complete list of these parameters and their distributions can be found in Table S11). Sensitivity analyses focused on wastewater sludge as a representative example. Specifically, we prescreened parameters using Spearman's rank order correlation coefficients with cost and carbon intensity indicators, where parameters with a p-value less than 0.05 and an absolute ρ-value larger than 0.1 were defined as the key drivers of uncertainty. Then, we performed Monte Carlo filtering with Kolmogorov−Smirnov test on identified key technological parameters (e.g., biocrude yield) to set targets for their future advancement by generating frequency distribution curves for each parameter for when the simulated MDSP was either higher or lower than the upper level of the market diesel price (5.81 $\$\cdot gal^{-1}$[42]). The value of the intersection of the two distribution curves represented the parameter value at which MDSP was equally likely to be above or below 5.81 $\$\cdot gal^{-1}$; this value was set as the target value these parameters need to reach to shift hydrothermally produced diesel toward financial viability. In a separate scenario analysis, we designed two alternative system configurations (Figure 1) to characterize the implications of these discrete choices: (alternative 1) removing the acid extraction step for phosphorus recovery or (alternative 2) adding a pressure swing adsorption unit for hydrogen recycling from hydrotreating gas products.

RESULTS AND DISCUSSION

Mass and Energy Flows. Mass flow rates of carbon, nitrogen, and phosphorus were strongly correlated to the biochemical composition of the feedstocks (Figure 2; elemental and biochemical compositions were represented as fractions of the ash-free dry weight). Among the five feedstocks for which compositional data were gathered from the literature, FOG—which was 91.2 to 100% lipid ($C_8H_{16}O$)[72]—had the highest carbon content (73.9% [67.4% to 80.2%]; 5th to 95th percentiles in brackets) and the highest unprocessed (i.e., feedstock) energy content (39.5 [35.5 to 43.2] $MJ\cdot kg^{-1}$, calculated based on eq S15). During the HTL reaction, lipids were mainly converted to medium- and long-chain fatty acids[73] and partitioned into the biocrude phase, while negligible amounts of off-gas, aqueous, and hydrochar byproducts were produced. As a result, 97.9% [82.6% to 100%] of carbon in FOG was transferred to biocrude for further hydrotreating and hydrocracking, leading to the highest energy recovery (54.8% [47.1% to 64.7%], the percentage of energy in feedstocks and hydrogen recovered in biofuels) among the evaluated feedstocks. In contrast, nitrogen recovery (the percentage of nitrogen in feedstocks recovered as fertilizers) from FOG was only 27.9% [13.5% to 39.7%] because a significant fraction of the feedstock nitrogen was simulated to partition into the biocrude phase and was lost to wastewater during subsequent hydrotreating. However, the system-level impacts of limited nitrogen recovery were minimal since the total nitrogen content in FOG was less than 0.20%. On the other end of the spectrum, only 40.7% [26.8% to 54.9%] of carbon in green waste was recovered in biocrude, and the total energy recovery was limited to 45.8% [30.7% to 58.5%]. This was due to the high (93.2% [90.2% to 96.3%]) carbohydrate content of green waste,[74,75] which led to the lowest carbon content (41.3% [37.8% to 44.8%]) and unprocessed energy content (11.4 [8.6 to 14.3] $MJ\cdot kg^{-1}$) among all feedstocks. As carbohydrate is readily decomposed into CO_2 off-gas and polar water-soluble molecules (e.g., methanol, ethanol[40]) which stay in the aqueous phase during hydrothermal conversion, a much smaller fraction of feedstock energy was recovered as biocrude (48.9% [31.9% to 66.5%] for green waste compared to 92.2% [78.5% to 100%] for FOG). Though the nitrogen recovery rate for green waste (83.6% [76.2% to 89.7%]) is the highest across the five feedstocks, the systems-level benefits can be negligible due to low total nitrogen content (0.78% [0.30% to 1.27%]). Sludge was the most protein rich (38% to 51%[22,76−78]) feedstock in this study and had the highest nutrient content (7.10% [6.30% to 8.15%] nitrogen and 2.74% [1.86% to 3.69%] phosphorus). After HTL, 71.7% [65.6% to 77.3%] of the total nitrogen was in the aqueous phase and primarily in the form of NH_4^+. The CHG unit process also mineralized aqueous organic nitrogen to NH_4^+. In the designed system, there were two mechanisms to recover nitrogen from the aqueous phase: (i) coprecipitation with phosphorus to form struvite ($MgNH_4PO_4{\cdot}6H_2O$) and (ii) membrane distillation and recovery in a sulfuric acid sweep solution to produce ammonium sulfate ($(NH_4)_2SO_4$). In the case of sludge, these two processes accounted for the fate of 11.8% [7.9% to 15.8%] and 59.3% [52.6% to 66.2%] of the nitrogen, respectively. The remaining nitrogen remained in the biocrude phase by forming indole, pyridine, pyrazine, and amine groups[73] and can be removed through hydrodenitrogenation reactions during hydrotreatment.[79] Though it was hard to recover this fraction of the nitrogen, efforts (e.g., sequential HTL, chemical washing off proteins from feedstock) have been made to redirect more nitrogen from biocrude to the HTL aqueous phase to reduce the burden of biocrude upgrading and also increase nitrogen-fertilizer production.[80−82] Phosphorus recovery (the percentage of phosphorus in feedstocks recovered as fertilizers) was high (>68% average phosphorus recovered) regardless of feedstock type, consistent with experimentally demonstrated phosphorus recovery.[17,83,84] However, the benefits of recovering phosphorus can be negligible if the feedstock is not phosphorus-rich (e.g., FOG, green waste). Detailed feedstock biochemical compositions and the modeled elemental (including carbon, nitrogen, and phosphorus) and energy flows can be found in Tables S1 and S12, respectively.

Sustainability Implications Across Feedstocks. *Waste Management Perspective.* In addition to feedstock properties, the financial viability and relative environmental sustainability

https://doi.org/10.1021/acs.est.3c07394
Environ. Sci. Technol. 2024, 58, 2528−2541

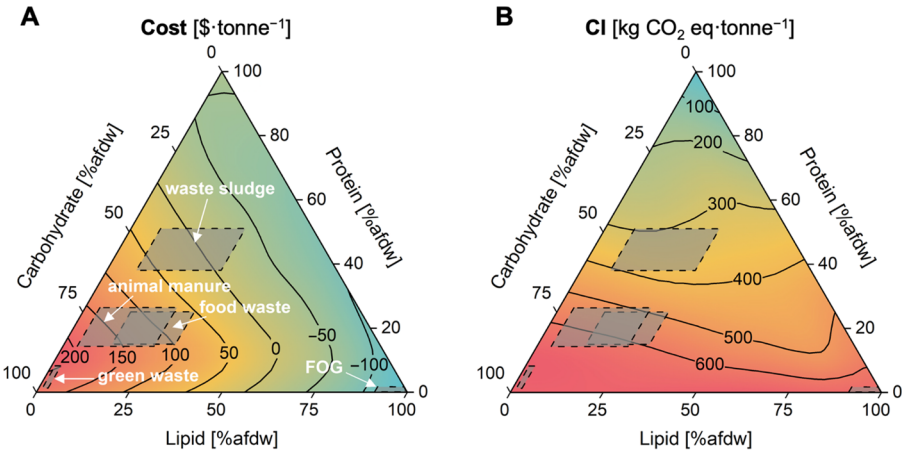

Figure 3. Waste management (A) cost and (B) carbon intensity (CI) for all combinations of biochemical compositions. A total of 66 biochemical compositions were simulated, with the median value of 1000 Monte Carlo simulations shown in the figure. A constant moisture content (80%) and a constant ash content (15%, on a dry weight basis) were assumed for each biochemical composition. Carbohydrate, lipid, and protein are reported on an ash-free dry weight basis. The biochemical compositions for each representative feedstock were (sludge) 8% to 30.8% lipid and 38 to 51% protein,[22,76−78] (FOG) 91.2% to 100% lipid and 0% to 1.2% protein,[72] (food waste) 13% to 30% lipid and 15% to 25% protein,[72] (green waste) 1.0% to 2.6% lipid and 1.6% to 8.2% protein,[74,75] and (animal manure) 3.8% to 24.7% lipid and 14.3% to 26.4% protein.[22,91] For all feedstocks, carbohydrate was calculated as 100%−lipid%−protein%.

of HTL-based valorization will also depend on the benchmark against which it is compared: for instance, whether the technology is being deployed by stakeholders primarily focused on waste management or renewable diesel production. In the context of waste management, we compared the cost and life cycle GHG emissions of the HTL-based process (simulated in this work) to current waste management practices (i.e., landfill, land application, incineration[9]) for the final management of residual biomass (Figure 2, right panels). As expected, the hydrothermal system was the most cost-effective for FOG management (−193 [−408 to −13.8] $·tonne^{-1}), while it was largely outcompeted by existing strategies for green waste management (251 [160 to 329] $·tonne^{-1}, compared to the current 53.9 to 165 $·tonne^{-1}[185]). These results suggest lipid-rich waste streams have the potential to generate significant revenue via hydrothermal systems whereas alternative management strategies should be considered for carbohydrate-rich waste (e.g., fermentation which aims for ethanol production[86]). For sludge, the cost of the hydrothermal system (33.0 [−77.2 to 121] $·tonne^{-1}) was generally below the lower end of the cost for existing management strategies: less expensive than land application (331 to 882 $·tonne^{-1}) and incineration (331 to 551 $·tonne^{-1}) but partially overlapping with landfill (110 to 717 $·tonne^{-1}).[9] Notably, approximately 32% of the simulated sludge management costs and 96% of simulated FOG costs were negative, suggesting that waste managers handling sludge and FOG could (in some cases) charge a hydrothermal plant for their renewable waste resources instead of paying a tipping fee. In addition, food waste has a hydrothermal management cost (86.4 [−44.6 to 185] $·tonne^{-1}) at the lower end of the current management strategies (40 to 400 $·tonne^{-1}[110]), while the cost for hydrothermal management of animal manure (158 [52.8 to 242] $·tonne^{-1}) is at the higher end of the current practices (6 to 165 $·tonne^{-1}[187]).

With regard to life cycle GHG emissions for wastewater sludge management, the hydrothermal system (367 [206 to 497] kg CO_2 eq·tonne^{-1}) had lower carbon intensity than landfilling (732 to 2200 kg CO_2 eq·tonne^{-1}[188]) and comparable values to incineration (−245 to 1450 kg CO_2 eq·tonne^{-1}[188]) and land application (150 to 715 kg CO_2 eq·tonne^{-1}[188]). No existing life cycle GHG emissions data were available for the other four wastes evaluated in this study. Similar to the trend observed for management cost, among these four wastes, FOG generated the lowest simulated carbon intensity (391 [162 to 628] kg CO_2 eq·tonne^{-1}), which was followed by food waste and animal manure (535 [359 to 695] kg CO_2 eq tonne^{-1} and 591 [477 to 704] kg CO_2 eq tonne^{-1}, respectively), while green waste demonstrated the highest carbon intensity (769 [651 to 901] kg CO_2 eq tonne^{-1}). Overall, the HTL-based resource recovery systems showed promising economic and environmental benefits, especially for feedstocks such as FOG and wastewater sludge.

As feedstocks for hydrothermal systems may be a mixture of several organic wastes, we further extended our analyses to examine across the spectrum of biochemical compositions (Figure 3). While a strong negative correlation between cost and feedstock lipid content was expected and observed, we also found protein was the strongest biochemical driver of carbon intensity. This was because protein content was directly associated with the total nitrogen content in the feedstock. Though a larger portion of nitrogen in protein-rich feedstocks may be transferred to biocrude due to intensified Maillard reaction,[89] a higher absolute mass of nitrogen in the aqueous phase (consistent with experimental data[34]) could led to greater production of ammonium sulfate and greater subsequent fertilizer offsets: the environmental benefits of this increased fertilizer production were more impactful than increased biofuel yields (which were impacted most significantly by lipid content). As a result, for waste streams comprised entirely of protein, the carbon intensity could reach a minimum value of 14.7 [−280 to 280] kg CO_2 eq·tonne^{-1}. In practice, cotreatment of different organic wastes could achieve greater economic scale and help mitigate the costs and CIs of carbohydrate-rich feedstocks.[31] For example, existing waste management infrastructure could serve as intermediate destinations for carbohydrate-rich feedstocks with later transport to an HTL-based system, where they can be comanaged

https://doi.org/10.1021/acs.est.3c07394
Environ. Sci. Technol. 2024, 58, 2528−2541

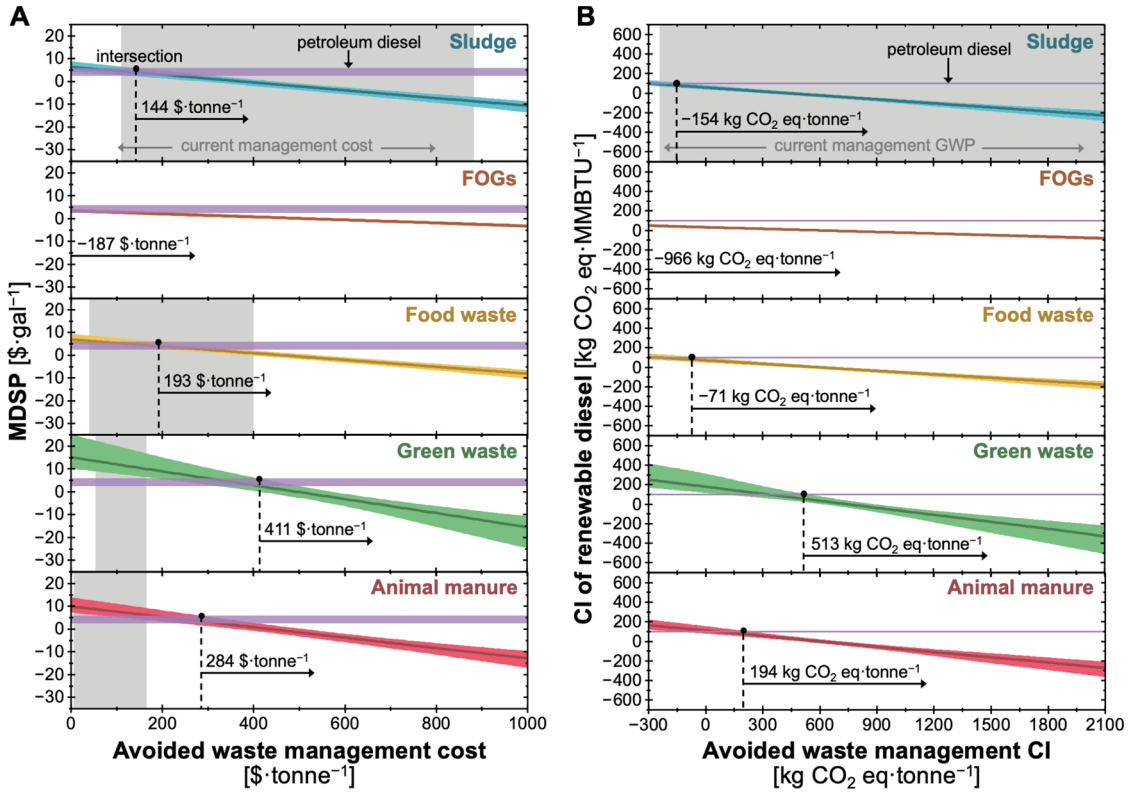

Figure 4. (Left) Minimum diesel selling price (MDSP) and (right) carbon intensity (CI) of HTL-based resource recovery systems for different feedstocks. Middle lines and the band represent 50th and 5th/95th percentiles of 1000 Monte Carlo simulations. Purple bands/lines indicate the market price of diesel (data from 2018 to 2022; 2.37 to 5.81 $·gal^{-1}[142]) in the left panel and petroleum diesel carbon intensity (101 kg CO_2 eq·MMBTU^{-1}[139]) in the right panel. Vertical dashed lines in all figures indicate the break-even point, where the 95th percentile of simulated HTL-based systems is equivalent to the upper level of the current diesel price or carbon intensity. Arrows are oriented to highlight the *x*-axis values that represent the opportunity space for the HTL-based system. Shaded areas represent the current management cost (left panel) and CI (right panel) for feedstocks. For CI of wastewater sludge, the gray shaded area only covers part of the current value (−245 to 2200 kg CO_2 eq·tonne^{-1}) for figure readability. Note as more negative avoided waste management costs and CI could be available for FOG, another version of this figure for FOG with extended *x*-axis (Figure S2) was included in the Supporting Information.

with locally produced feedstocks with higher lipid or protein content. Ultimately, HTL-based systems could be deployed to manage regionally relevant combinations of waste resources. Through locality-specific optimization of HTL-based resource recovery, regional organic waste management systems could be optimized to reduce or eliminate specific waste management practices (e.g., by replacing aging incinerators[90]) and support broader benefits for communities.

Renewable Diesel Producer Perspective. Given that HTL-based systems have the potential to support biofuel production, we also characterized the cost and life cycle GHG emissions of HTL-based renewable diesel production (simulated in this work) from the perspective of a fuel producer and benchmarked it against fossil-based diesel production (from the literature; Figure 4). In the case of sludge, MDSP and carbon intensity for produced renewable diesel were estimated to be 6.39 [4.42 to 8.78] $·gal^{-1} and 98.5 [75.0 to 132] kg CO_2 eq·MMBTU^{-1} if we do not consider offsetting current sludge management costs and environmental impacts. However, the fuel producer would be providing a waste management service that could have an associated fee and offset the life cycle GHG emissions of the current waste disposal route. If waste managers paid at least 144 $·tonne^{-1} in management costs for sludge disposal (to the fuel producer) and at least −154 kg CO_2 eq·tonne^{-1} of carbon offsets were allocated to the fuel producer (both of which are toward the low end of typical costs [110 to 882 $·tonne^{-1}, Figure 4] and emissions [−245 to 2200 kg CO_2 eq·tonne^{-1}, Figure 4] of sludge management), the MDSP and carbon intensity of renewable diesel would be comparable to petroleum diesel (Figure 4). Similarly, fuel producers can charge a similar price to traditional management methods for food waste (193 $·tonne^{-1} compared to the current range of 40 to 400 $·tonne^{-1}[110]) to achieve a cost competitive fuel. For FOG, our analysis has shown that there is no need to charge any fee for financially viable renewable diesel production (Figure 4). However, FOG has been commoditized and the fuel producer may need to purchase FOG at additional expenditure.[87,92] In that case, the more negative avoided management cost and carbon intensity can make HTL-based renewable diesel production less competitive (Figure S2). Alternatively, a fuel producer would need to charge green waste generators at least 411 $·tonne^{-1} to produce a cost competitive fuel, which is significantly higher than current management costs (53.9 to 165 $·tonne^{-1}).[85] In all cases, findings related to financial viability to HTL-supported renewable diesel are sensitive to assumptions of IRR, and perceived risks could increase the necessary IRR to garner investment, which would subsequently increase MDSP values. Thus, it is important to identify the key contributors to the cost and carbon intensity of hydrothermal systems and further improve its competitiveness.

https://doi.org/10.1021/acs.est.3c07394
Environ. Sci. Technol. 2024, 58, 2528−2541

Cost and Carbon Intensity Drivers. Based on the potential environmental and economic benefits of wastewater sludge valorization with the HTL-based process, we used this feedstock as an example to systematically identify the key drivers of cost and environmental impacts of the system and to provide targeted guidance for future research and development. Across the HTL-based process, CHP was the most capital-intensive unit, accounting for 34.2% [28.4% to 41.1%] of the total installed cost (TIC, 32.7 [29.2 to 37.1] MM$ [million dollar]), followed by HTL (23.6% [18.6% to 28.2%]) (Figure S3A). In our system, the installed cost of the HTL reactor and its auxiliary units (e.g., reactor heater, knockout drums, solids filter) was estimated to be 7.7 MM$ (Table S8). This value is lower than the reported HTL installed cost in Snowden-Swan et al. (15.9 MM$, excluding dewatering, HTL aqueous phase recycle, and balance of plant to be consistent with our design).[22] This difference is largely explained by our attribution of the steam generators and heat oil systems (estimated to be 4.7 MM$ in our system) to a centralized heating utility generation system (i.e., CHP), rather than the HTL unit. Through sensitivity analysis, the uncertainty in the capital cost of the HTL reactor (Table S11) was not identified as a key cost driver of uncertainty in cost and CI indicators (i.e., it did not meet the criteria to be included in Table S13). For the material cost, hydrotreating and hydrocracking were the largest contributors (representing 52.3% [40.9% to 62.8%] combined) because of H_2 costs. However, most of the H_2 was not consumed and represented 90% v/v of the off-gas from hydrotreating and hydrocracking, indicating that the plant could benefit from recycling this stream (discussed as Alternative 2 in the following section). Nutrient recovery also consumed a large amount of chemicals including H_2SO_4 and $MgCl_2$, accounting for a combined total of 28.7% [20.5% to 39.1%] of the total material cost. HTL and CHG were the two most predominate utility users, accounting for 41.6% [40.2% to 43.0%] and 42.6% [44.7% to 47.1%] of the system heating needs and 38.3% [36.7% to 39.9%] and 43.1% [40.8% to 45.5%] of the cooling demand, respectively. However, due to heat integration, 63.0% [62.5% to 63.4%] of the system heating and 59.7% [58.9% to 60.8%] of the cooling could be offset through heat exchange (pinch analysis in Figure S1).

With regard to environmental impacts, the construction phase accounted for a total of 5.1 [4.7 to 5.5] k-tonne CO_2 eq (k-tonne: thousand tonne), with the HTL part (including HTL reactors and other auxiliary units such as pumps and reactor heaters) accounting for more than half of the total construction emissions (60.3% [56.8% to 62.9%]). This was due to a large amount of stainless steel needed to withstand the high pressure, temperature, and loading rate of the HTL reactor and the fact that heat exchangers for HTL are often overdesigned to overcome the plugging issue due to the high viscosity of the feedstock.[50] To reduce this source of environmental impacts, an innovative HTL-based system called Flashing for Low-fouling, Steam-based Heat recovery in Hydrothermal Liquefaction (FLASH-HTL) has been under development to eliminate the HTL heat exchanger and reduce the associated environmental impacts and cost.[93] Beyond the HTL reactor and associated units, CHP was responsible for 18.5% [15.6% to 22.7%] of the GHG emissions from the construction phase, which was consistent with its high construction cost. However, when the heating and electricity offsets were considered (as describe in the System Description section), the net contribution of CHP to the carbon intensity of the system was largely negative (−90 [−230 to 18] k-tonne CO_2 eq over 30 years). The system products also yielded GHG offsets, with the produced biofuels yielding −1.7 [−2.9 to −0.4] k-tonne CO_2 eq·yr^{-1} and fertilizer substitutes yielding −4.9 [−7.0 to −2.8] k-tonne CO_2 eq·yr^{-1}. Utility consumption was again an important factor, responsible for 15.6 [11.1 to 18.8] k-tonne CO_2 eq·yr^{-1} with CHG and HTL as the two major utility users in the system.

In addition to cost and life cycle GHG breakdown, we also leveraged Spearman's rank of order correlation coefficients to prescreen all uncertain parameters (Table S11) for the wastewater sludge case. Key parameters identified by the analysis could be categorized into distinct groups of contextual parameters and technological parameters, the latter of which was broken into subcategories based on the relevant unit operation (Table S13). Further analyses were included to discuss these parameters based on their subcategory.

Opportunities to Advance the Sustainability of the HTL-Based Resource Recovery System. *Navigating Nutrient and Hydrogen Recovery.* In exploring the impacts of potential system design, we included two alternative system configurations and compared their costs and environmental impacts to the baseline design. For nutrient recovery, we removed the acid extraction step (thus phosphorus in the hydrochar would not be recovered; Alternative 1, Figure 1) and assumed hydrochar to be a neutral end-product (i.e., not generating value or environmental offsets). With these modifications, the sludge management cost increased to 72.7 [−32.1 to 154] $·tonne^{-1} (vs a median cost of 33.0 $·tonne^{-1} of the baseline system) due to less material input for struvite production (Figure S4A) but improved the environmental performance of the system (carbon intensity decreased to 275 [113 to 408] kg CO_2 eq·tonne^{-1}). This indicated the life cycle GHG emissions associated with the chemicals (e.g., H_2SO_4, $MgCl_2$) input for struvite precipitation were more significant than the benefit of recovering phosphorus (Figure S4B), revealing the cost-environmental impact trade-off on nutrient recovery from hydrochar. To reduce these costs, alternative chemical sources (e.g., magnesium from seawater or brine[94]) can be used, but the quality of products may be compromised.[94]

Given that our analysis identified H_2 as a major cost contributor, we designed an alternative system by adding a pressure swing adsorption (PSA) unit to recycle the H_2 vented from hydrotreating (Alternative 2, Figure 1). Compared to the baseline design, up to 90% of the hydrogen can be reused, significantly reducing material costs and CHP TIC (as a smaller CHP unit was needed to burn less fuel gas; Figure S5A), although less GHG credit was produced in CHP (due to less electricity production; Figure S5B). Collectively, this alternative configuration led to a decreased management cost of −1.11 [−108 to 93.1] $·tonne^{-1} with 50.8% of simulations being negative, but an increased carbon intensity (457 [366 to 553] kg CO_2 eq·tonne^{-1}) compared to the baseline design.

Deployment Considerations for Waste Valorization. The loading rate of feedstocks (100 dry tonne·day^{-1})—which is, for example, equivalent to the food waste of around 337,000 people (assuming 0.279 kg food waste·capita^{-1}·day^{-1})[95] or wastewater sludge from a water resource recovery facility (WRRF; a.k.a. wastewater treatment plant, WWTP) of around 100 million gallon per day (MGD)—significantly affected the relative sustainability of the HTL-based waste management system. Taking sludge as an example, we varied the WRRF size

https://doi.org/10.1021/acs.est.3c07394
Environ. Sci. Technol. 2024, 58, 2528−2541

from 20 to 320 MGD (Figure S6). Although carbon intensity remained stable (median value between 351 to 397 kg CO_2 eq·tonne^{-1}), the sludge management cost varied from 815 [659 to 971] $·tonne^{-1} (at 20 MGD) to −99.4 [−213 to 0.9] $·tonne^{-1} (at 320 MGD). Therefore, from an economic perspective, the system size is a critical factor in determining the location specific viability of hydrothermal HTL-based systems.

Due to the large capital investment for the HTL-based plant (with a TIC of 32.7 [29.2 to 37.1] MM$), the IRR was another parameter that significantly affected the system's economic performance (but not life cycle carbon intensity; Figure S7A). In our study, we assumed different IRR ranges for waste management and renewable diesel production based on potential financing mechanisms. For waste management, a low IRR (0% to 5%) could be achieved through the State Revolving Loan Fund,[67,68] for instance. The management cost for wastewater sludge varied from 7.3 [−117 to 96.2] $·tonne^{-1} at a 0% IRR to 64.8 [−49.6 to 158] $·tonne^{-1} at a 5% IRR (Figure S7A), demonstrating consistent economic benefits over traditional management methods. However, IRR can be higher when evaluating the system from the biofuel production perspective (5% to 15%) because financing may rely on venture capital. Increasing IRR increased MDSP from 5.25 [3.59 to 7.14] $·gal^{-1} at a 5% IRR to 7.51 [5.70 to 10.1] $·gal^{-1} at a 15% IRR (Figure S7A), with the latter mostly higher than the commercial diesel price range. Therefore, the accessibility to low interest capital can be a critical factor in determining the financial viability of HTL-based systems, especially when the target is biofuel production.

Technology Targets for Financially Viable Renewable Diesel Production. To better understand the implications of key technological parameters on the financial viability of the HTL-based process, we performed Monte Carlo filtering (Figure 5) to quantitatively set explicit targets using the upper level of the commercial diesel price (5.81 $·gal^{-1}) as the threshold while assuming a sludge management cost of 0. In other words, we determined the target value each parameter needs to reach for the produced renewable diesel to have a greater likelihood (than not) of being in the price range of commercial diesel (i.e., the arrow pointed sides of the blue and red lines cross in Figure 5) without cost offsets paid by wastewater sludge generators. The technological parameters evaluated included HTL biocrude yield, HTL aqueous yield, and hydrotreating yield; these parameters were selected due to their strong influence on MDSP, as identified in the Spearman's rank order correlation results (Table S13). Among these three parameters, HTL biocrude yield was a key driver of uncertainty (Kolmogorov−Smirnov test $p = 1.37 \times 10^{-15}$). When it reached the target of >0.440, the MDSP decreased to 5.58 [4.10 to 7.73] $·gal^{-1}, with 56.6% of the samples having a MDSP lower than the upper level of commercial diesel price. Recent experimental observations have reported HTL biocrude yields from 0.094[96] to 0.44[22] for wastewater sludge, only with the higher end approaching the target. Future research may include the use of acid or alkaline catalyst[97] or optimize the separation across the HTL phases to further improve the biocrude yields and increase the financial viability of the HTL-based process. For the other two parameters (HTL aqueous yield and hydrotreating yield), though they were identified as key drivers, experimental works have demonstrated performance that already exceeds the proposed targets: HTL aqueous yield target of 0.254, with

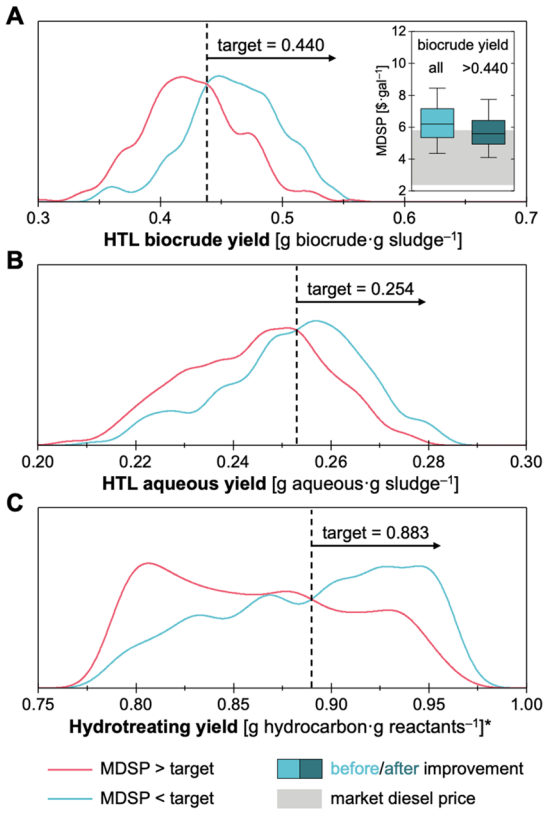

Figure 5. Monte Carlo filtering results for technological parameters that had a Kolmogorov−Smirnov test $p < 0.05$ for MDSP, including (A) the yield of biocrude from the feedstock during hydrothermal liquefaction (HTL), (B) the yield of aqueous phase from the feedstock during HTL, and (C) the yield of hydrocarbons from biocrude and hydrogen during hydrotreating. The lines represent the distribution of corresponding parameters when the simulated minimum diesel selling price (MDSP) was (blue) lower or (red) higher than the upper level of the price threshold (set as the maximum market price of diesel from 2018 to 2022; 5.81 $·gal^{-1}[142]), respectively. The "target" values identified represent the parameter value at which the simulated MDSP is equally likely to be above or below the price threshold. The black arrows indicate the research direction in which each parameter could further lower the MDSP. Box plots in (A) compare the MDSP with (light blue) baseline assumptions to MDSP if (dark blue) parameter targets are achieved. The whiskers, boxes, and midline of the box plots represented 5th/95th, 25th/75th, and 50th percentiles, respectively. Gray shaded areas indicate the market price of diesel (data from 2018 to 2022; 2.37 to 5.81 $·gal^{-1}[142]). *Reactants in hydrotreating include biocrude and hydrogen.

reported achievements up to 0.36,[22] and hydrotreating yield target of 0.883, with reported achievements of 0.82 to 0.95[22,98−100]). Although further improvements beyond these experimentally demonstrated results will have a marginal benefit in terms of achieving MDSPs below the threshold value, they will continue to improve resource recovery potential, drive down costs, and increase the financial viability of the system.

OPPORTUNITIES AND CHALLENGES

As we pursue a more circular economy, HTL-based waste valorization systems could help close the supply chain loop by converting organic wastes to biofuels and fertilizers. In this study, we systematically evaluated the economic and environ-

https://doi.org/10.1021/acs.est.3c07394
Environ. Sci. Technol. 2024, 58, 2528−2541

mental sustainability of hydrothermal systems across all feasible feedstock biochemical compositions. The results demonstrated that lipid- and protein-rich feedstocks can reduce management costs and environmental impacts. But for carbohydrate-rich feedstocks like green waste, even without considering degradation-resistant lignin, higher costs and environmental impacts were predicted. Moreover, by considering alternative system configurations, we found that both phosphorus recovery from hydrochar and hydrogen recycling from hydrotreating can lower costs but at the expense of higher environmental impacts. Finally, through sensitivity analyses, we set specific targets (i.e., increasing the wastewater sludge-biocrude yield to 0.440) for future research and development.

While promising, there are still challenges for the practical implementation of HTL-based treatment systems. For example, recovered fertilizers from this study were assumed to be sold at their market prices. However, public reluctance to use "waste-derived" fertilizers may lead to a lower selling price and undermine the financial standing of the HTL-based system. Also, energy-dense feedstocks such as FOG have become commoditized within some industries and in some localities.[87,92] To characterize the implications of FOG supply incurring costs, we repeated our analysis in Figure 4 for avoided waste management costs to −600 $·tonne^{-1} (i.e., a FOG purchase cost up to 600 $·tonne^{-1}[87]) and found a purchase cost more than 187 $·tonne^{-1} resulted in the cost of produced diesel higher than the market diesel price range (Figure S2). However, as some amounts of FOG from much smaller, distributed sources (as opposed to, for example, rendering plants) are still disposed of landfills or incinerated,[92] or are sent to municipal WRRFs,[101] shifting this part of FOG to be the feedstock for the HTL-based system (assuming free of charge, Figure S2) could be financially viable. Therefore, the ultimate decision to deploy HTL-based valorization systems should be guided by locality-specific evaluations, replacing the full ranges evaluated here with more specific contextual parameters and logistical considerations,[71] while paying special attention to highly sensitive parameters like waste types, quantities, and market dynamics as identified in this work.

To offer further economic and environmental incentives for HTL-based waste management, alternative HTL product targets, unit operations, and treatment benefits can be explored. For instance, HTL could produce propylene—an important industrial precursor—from polyhydroxybutyrate (PHB)-enriched biomass relevant to wastewater treatment operations.[102] For lignin-rich feedstocks, the HTL process can be optimized for polyols (precursors of polyurethane) production.[103] In addition, HTL-derived hydrochar could be a potential solid fuel after acid leaching,[104] and beyond struvite, the phosphorus extracted could be recovered as calcium phosphate[105] or hydroxyapatite.[84] Further, the HTL aqueous phase could also be used for the cultivation of algae and/or bacteria after proper pretreatment (e.g., partial oxidation, nanofiltration, adsorption) removing inhibiting compounds,[106] or be recirculated to the HTL influent as the reaction solvent to improve biocrude production.[82] In terms of additional treatment benefits, the HTL-based system could also offer a value proposition with the destruction of recalcitrant contaminants. In particular, recent experimental results have demonstrated HTL could destroy >99% of all tested PFAS under alkaline conditions within 30 min.[19] As experimental data become available, additional units (e.g., for higher value product synthesis and separations) or relationships (e.g., dependency of PFAS destruction on HTL temperature and reaction time) can be integrated in QSDsan and considered in future TEA and LCA studies to set technology targets and prioritize the research, development, and deployment (RD&D) of HTL-based resource recovery systems.

■ ASSOCIATED CONTENT

Supporting Information

The Supporting Information is available free of charge at https://pubs.acs.org/doi/10.1021/acs.est.3c07394.

> Feedstock characterization, detailed system design and process conditions, key equipment cost, detailed TEA and LCA assumptions and parameters, selection of uncertainty distributions, pinch analysis results, renewable diesel production using FOG as the feedstock, cost and environmental impact breakdown for alternative system configurations, effects of contextual parameters, supplementary uncertainty and sensitivity analyses results, supplementary elemental flow data, and LCA results for environmental impact indicators other than life cycle GHG emissions (PDF)

■ AUTHOR INFORMATION

Corresponding Author

Jeremy S. Guest − *Department of Civil and Environmental Engineering and Institute for Sustainability, Energy, and Environment, University of Illinois Urbana−Champaign, Urbana, Illinois 61801, United States;* orcid.org/0000-0003-2489-2579; Phone: (217) 244-9247; Email: jsguest@illinois.edu

Authors

Jianan Feng − *Department of Civil and Environmental Engineering, University of Illinois Urbana−Champaign, Urbana, Illinois 61801, United States;* orcid.org/0000-0001-6987-1187

Yalin Li − *Department of Civil and Environmental Engineering, Rutgers, The State University of New Jersey, Piscataway, New Jersey 08854, United States;* orcid.org/0000-0002-8863-4758

Timothy J. Strathmann − *Department of Civil and Environmental Engineering, Colorado School of Mines, Golden, Colorado 80401, United States;* orcid.org/0000-0002-7299-3115

Complete contact information is available at: https://pubs.acs.org/10.1021/acs.est.3c07394

Notes

The authors declare no competing financial interest.

■ ACKNOWLEDGMENTS

The authors would like to acknowledge Dr. Xinyi (Joy) Zhang (University of Illinois Urbana−Champaign) for assistance with the model development in QSDsan and the discussion about Monte Carlo filtering. This publication is based on research funded by the National Science Foundation (NSF) Awards CBET-2207191 and CBET-2207235.

REFERENCES

(1) *Biofuels and Bioproducts from Wet and Gaseous Waste Streams: Challenges and Opportunities*; United States Department of Energy, 2017.

(2) *Downstream Management of Organic Waste in the United States: Strategies for Methane Mitigation*; United States Environmental Protection Agency, 2022.

(3) Yusof, N.; Haraguchi, A.; Hassan, M. A.; Othman, M. R.; Wakisaka, M.; Shirai, Y. Measuring Organic Carbon, Nutrients and Heavy Metals in Rivers Receiving Leachate from Controlled and Uncontrolled Municipal Solid Waste (MSW) Landfills. *Waste Manag.* **2009**, *29* (10), 2666−2680.

(4) Liang, Y.; Xu, D.; Feng, P.; Hao, B.; Guo, Y.; Wang, S. Municipal Sewage Sludge Incineration and Its Air Pollution Control. *J. Clean. Prod.* **2021**, *295*, No. 126456.

(5) Kang, M.; Naushad, S.; Hartke, A.; Firth, I.; Madey, E.; Ogunremi, D.; Huang, H. Antibiotic Resistomes and Microbial Communities in Biosolid Fertilizers Collected from Two Canadian Wastewater Treatment Plants in a 10-Years Interval-Potential Risks to Food Chains? *Front. Food Sci. Technol.* **2022**, *2*, No. 894671.

(6) Mays, C.; Garza, G. L.; Waite-Cusic, J.; Radniecki, T. S.; Navab-Daneshmand, T. Impact of Biosolids Amendment and Wastewater Effluent Irrigation on Enteric Antibiotic-Resistant Bacteria − a Greenhouse Study. *Water Res. X* **2021**, *13*, No. 100119.

(7) Yakamercan, E.; Ari, A.; Aygün, A. Land Application of Municipal Sewage Sludge: Human Health Risk Assessment of Heavy Metals. *J. Clean. Prod.* **2021**, *319*, No. 128568.

(8) Johnson, G. R. PFAS in Soil and Groundwater Following Historical Land Application of Biosolids. *Water Res.* **2022**, *211*, No. 118035.

(9) Peccia, J.; Westerhoff, P. We Should Expect More out of Our Sewage Sludge. *Environ. Sci. Technol.* **2015**, *49* (14), 8271−8276.

(10) Bastidas-Oyanedel, J.-R.; Schmidt, J. E. Increasing Profits in Food Waste Biorefinery—A Techno-Economic Analysis. *Energies* **2018**, *11* (6), 1551.

(11) Gollakota, A. R. K.; Kishore, N.; Gu, S. A Review on Hydrothermal Liquefaction of Biomass. *Renew. Sustain. Energy Rev.* **2018**, *81*, 1378−1392.

(12) Jasiūnas, L.; Pedersen, T. H.; Toor, S. S.; Rosendahl, L. A. Biocrude Production via Supercritical Hydrothermal Co-Liquefaction of Spent Mushroom Compost and Aspen Wood Sawdust. *Renew. Energy* **2017**, *111*, 392−398.

(13) Ciuffi, B.; Loppi, M.; Rizzo, A. M.; Chiaramonti, D.; Rosi, L. Towards a Better Understanding of the HTL Process of Lignin-Rich Feedstock. *Sci. Rep.* **2021**, *11* (1), 15504.

(14) Li, Y.; Tarpeh, W. A.; Nelson, K. L.; Strathmann, T. J. Quantitative Evaluation of an Integrated System for Valorization of Wastewater Algae as Bio-Oil, Fuel Gas, and Fertilizer Products. *Environ. Sci. Technol.* **2018**, *52* (21), 12717−12727.

(15) Leow, S.; Shoener, B. D.; Li, Y.; DeBellis, J. L.; Markham, J.; Davis, R.; Laurens, L. M. L.; Pienkos, P. T.; Cook, S. M.; Strathmann, T. J.; Guest, J. S. A Unified Modeling Framework to Advance Biofuel Production from Microalgae. *Environ. Sci. Technol.* **2018**, *52* (22), 13591−13599.

(16) Zhu, Y.; Schmidt, A.; Valdez, P.; Snowden-Swan, L.; Edmundson, S. *Hydrothermal Liquefaction and Upgrading of Wastewater-Grown Microalgae: 2021 State of Technology*; PNNL-32695; US Department of Energy, 2022; No. 1855835. DOI: 10.2172/1855835.

(17) Ovsyannikova, E.; Kruse, A.; Becker, G. C. Feedstock-Dependent Phosphate Recovery in a Pilot-Scale Hydrothermal Liquefaction Bio-Crude Production. *Energies* **2020**, *13* (2), 379.

(18) Yu, J.; Nickerson, A.; Li, Y.; Fang, Y.; Strathmann, T. J. Fate of Per- and Polyfluoroalkyl Substances (PFAS) during Hydrothermal Liquefaction of Municipal Wastewater Treatment Sludge. *Environ. Sci. Water Res. Technol.* **2020**, *6* (5), 1388−1399.

(19) Hao, S.; Choi, Y.-J.; Wu, B.; Higgins, C. P.; Deeb, R.; Strathmann, T. J. Hydrothermal Alkaline Treatment for Destruction of Per- and Polyfluoroalkyl Substances in Aqueous Film-Forming Foam. *Environ. Sci. Technol.* **2021**, *55* (5), 3283−3295.

(20) Fan, Y.; Hornung, U.; Dahmen, N. Hydrothermal Liquefaction of Sewage Sludge for Biofuel Application: A Review on Fundamentals, Current Challenges and Strategies. *Biomass Bioenergy* **2022**, *165*, No. 106570.

(21) Silva Thomsen, L. B.; Carvalho, P. N.; dos Passos, J. S.; Anastasakis, K.; Bester, K.; Biller, P. Hydrothermal Liquefaction of Sewage Sludge; Energy Considerations and Fate of Micropollutants during Pilot Scale Processing. *Water Res.* **2020**, *183*, No. 116101.

(22) Snowden-Swan, L. J.; Li, S.; Thorson, M. R.; Schmidt, A. J.; Cronin, D. J.; Zhu, Y.; Hart, T. R.; Santosa, D. M.; Fox, S. P.; Lemmon, T. L.; Swita, M. S. *Wet Waste Hydrothermal Liquefaction and Biocrude Upgrading to Hydrocarbon Fuels: 2022 State of Technology*; PNNL-33622; Pacific Northwest National Lab. (PNNL): Richland, WA, United States, 2022. DOI: 10.2172/1897670.

(23) Singh, D.; Jiang, X.; Jankovic, M.; Toll, F. Improving Yields, Compatibility and Tailoring the Properties of Hydrothermal Liquefaction Bio-Crude Using Yellow Grease. *Fuel* **2023**, *344*, No. 128066.

(24) Cronin, D.; Schmidt, A. J.; Billing, J.; Hart, T. R.; Fox, S. P.; Fonoll, X.; Norton, J.; Thorson, M. R. Comparative Study on the Continuous Flow Hydrothermal Liquefaction of Various Wet-Waste Feedstock Types. *ACS Sustain. Chem. Eng.* **2022**, *10* (3), 1256−1266.

(25) Aierzhati, A.; Stablein, M. J.; Wu, N. E.; Kuo, C.-T.; Si, B.; Kang, X.; Zhang, Y. Experimental and Model Enhancement of Food Waste Hydrothermal Liquefaction with Combined Effects of Biochemical Composition and Reaction Conditions. *Bioresour. Technol.* **2019**, *284*, 139−147.

(26) Motavaf, B.; Savage, P. E. Effect of Process Variables on Food Waste Valorization via Hydrothermal Liquefaction. *ACS EST Eng.* **2021**, *1* (3), 363−374.

(27) Posmanik, R.; Martinez, C. M.; Cantero-Tubilla, B.; Cantero, D. A.; Sills, D. L.; Cocero, M. J.; Tester, J. W. Acid and Alkali Catalyzed Hydrothermal Liquefaction of Dairy Manure Digestate and Food Waste. *ACS Sustain. Chem. Eng.* **2018**, *6* (2), 2724−2732.

(28) Conti, F.; Toor, S. S.; Pedersen, T. H.; Seehar, T. H.; Nielsen, A. H.; Rosendahl, L. A. Valorization of Animal and Human Wastes through Hydrothermal Liquefaction for Biocrude Production and Simultaneous Recovery of Nutrients. *Energy Convers. Manag.* **2020**, *216*, No. 112925.

(29) Lu, J.; Watson, J.; Zeng, J.; Li, H.; Zhu, Z.; Wang, M.; Zhang, Y.; Liu, Z. Biocrude Production and Heavy Metal Migration during Hydrothermal Liquefaction of Swine Manure. *Process Saf. Environ. Prot.* **2018**, *115*, 108−115.

(30) Cao, L.; Luo, G.; Zhang, S.; Chen, J. Bio-Oil Production from Eight Selected Green Landscaping Wastes through Hydrothermal Liquefaction. *RSC Adv.* **2016**, *6* (18), 15260−15270.

(31) LeClerc, H. O.; Page, J. R.; Tompsett, G. A.; Niles, S. F.; McKenna, A. M.; Valla, J. A.; Timko, M. T.; Teixeira, A. R. Emergent Chemical Behavior in Mixed Food and Lignocellulosic Green Waste Hydrothermal Liquefaction. *ACS Sustain. Chem. Eng.* **2023**, *11* (6), 2427−2439.

(32) Ellersdorfer, M. Hydrothermal Co-Liquefaction of Chlorella Vulgaris with Food Processing Residues, Green Waste and Sewage Sludge. *Biomass Bioenergy* **2020**, *142*, No. 105796.

(33) Leow, S.; Witter, J. R.; Vardon, D. R.; Sharma, B. K.; Guest, J. S.; Strathmann, T. J. Prediction of Microalgae Hydrothermal Liquefaction Products from Feedstock Biochemical Composition. *Green Chem.* **2015**, *17* (6), 3584−3599.

(34) Li, Y.; Leow, S.; Fedders, A. C.; Sharma, B. K.; Guest, J. S.; Strathmann, T. J. Quantitative Multiphase Model for Hydrothermal Liquefaction of Algal Biomass. *Green Chem.* **2017**, *19* (4), 1163−1174.

(35) Obeid, R.; Smith, N.; Lewis, D. M.; Hall, T.; van Eyk, P. A Kinetic Model for the Hydrothermal Liquefaction of Microalgae, Sewage Sludge and Pine Wood with Product Characterisation of Renewable Crude. *Chem. Eng. J.* **2022**, *428*, No. 131228.

(36) Qian, L.; Wang, S.; Savage, P. E. Fast and Isothermal Hydrothermal Liquefaction of Sludge at Different Severities: Reaction

Products, Pathways, and Kinetics. *Appl. Energy* **2020**, *260*, No. 114312.
(37) Masoumi, S.; Dalai, A. K. Techno-Economic and Life Cycle Analysis of Biofuel Production via Hydrothermal Liquefaction of Microalgae in a Methanol-Water System and Catalytic Hydrotreatment Using Hydrochar as a Catalyst Support. *Biomass Bioenergy* **2021**, *151*, No. 106168.
(38) Summers, H. M.; Ledbetter, R. N.; McCurdy, A. T.; Morgan, M. R.; Seefeldt, L. C.; Jena, U.; Kent Hoekman, S.; Quinn, J. C. Techno-Economic Feasibility and Life Cycle Assessment of Dairy Effluent to Renewable Diesel via Hydrothermal Liquefaction. *Bioresour. Technol.* **2015**, *196*, 431−440.
(39) Pegallapati, A. K.; Dunn, J. B.; Frank, E. D.; Jones, S.; Zhu, Y.; Snowden-Swan, L.; Davis, R.; Kinchin, C. M. *Supply Chain Sustainability Analysis of Whole Algae Hydrothermal Liquefaction and Upgrading*; ANL/ESD-15/8; US Department of Energy, 2015; No. 1183770. DOI: 10.2172/1183770.
(40) Jones, S. B.; Zhu, Y.; Anderson, D. B.; Hallen, R. T.; Elliott, D. C.; Schmidt, A. J.; Albrecht, K. O.; Hart, T. R.; Butcher, M. G.; Drennan, C.; Snowden-Swan, L. J.; Davis, R.; Kinchin, C. *Process Design and Economics for the Conversion of Algal Biomass to Hydrocarbons: Whole Algae Hydrothermal Liquefaction and Upgrading*; PNNL-23227; US Department of Energy, 2014; No. 1126336. DOI: 10.2172/1126336.
(41) DeRose, K.; DeMill, C.; Davis, R. W.; Quinn, J. C. Integrated Techno Economic and Life Cycle Assessment of the Conversion of High Productivity, Low Lipid Algae to Renewable Fuels. *Algal Res.* **2019**, *38*, No. 101412.
(42) *Gasoline and Diesel Fuel Update*. https://www.eia.gov/petroleum/gasdiesel/index.php (accessed 2023-03-14).
(43) Aierzhati, A.; Watson, J.; Si, B.; Stablein, M.; Wang, T.; Zhang, Y. Development of a Mobile, Pilot Scale Hydrothermal Liquefaction Reactor: Food Waste Conversion Product Analysis and Techno-Economic Assessment. *Energy Convers. Manag. X* **2021**, *10*, No. 100076.
(44) Jiang, Y.; Mevawala, C.; Li, S.; Schmidt, A.; Billing, J.; Thorson, M.; Snowden-Swan, L. Uncertainty Analysis for Techno-Economic and Life-Cycle Assessment of Wet Waste Hydrothermal Liquefaction with Centralized Upgrading to Produce Fuel Blendstocks. *J. Environ. Chem. Eng.* **2023**, *11* (3), No. 109706.
(45) Li, Y.; Zhang, X.; Morgan, V. L.; Lohman, H. A. C.; Rowles, L. S.; Mittal, S.; Kogler, A.; Cusick, R. D.; Tarpeh, W. A.; Guest, J. S. QSDsan: An Integrated Platform for Quantitative Sustainable Design of Sanitation and Resource Recovery Systems. *Environ. Sci. Water Res. Technol.* **2022**, *8*, 2289.
(46) QSD-Group/EXPOsan at 2c9e246bb19cb67b8f8ac52ec4b978b2b118d12a. *GitHub*. https://github.com/QSD-Group/EXPOsan/tree/2c9e246bb19cb67b8f8ac52ec4b978b2b118d12a (accessed 2023-11-06).
(47) Cortes-Peña, Y.; Kumar, D.; Singh, V.; Guest, J. S. BioSTEAM: A Fast and Flexible Platform for the Design, Simulation, and Techno-Economic Analysis of Biorefineries under Uncertainty. *ACS Sustain. Chem. Eng.* **2020**, *8* (8), 3302−3310.
(48) GitHub - BioSTEAMDevelopmentGroup/biosteam at 0da3da0165078bbafea15caef70b17cfa40616e6. GitHub. https://github.com/BioSTEAMDevelopmentGroup/biosteam (accessed 2023−11−06).
(49) Elliott, D. C.; Biller, P.; Ross, A. B.; Schmidt, A. J.; Jones, S. B. Hydrothermal Liquefaction of Biomass: Developments from Batch to Continuous Process. *Bioresour. Technol.* **2015**, *178*, 147−156.
(50) Knorr, D.; Lukas, J.; Schoen, P. *Production of Advanced Biofuels via Liquefaction - Hydrothermal Liquefaction Reactor Design: April 5, 2013*; NREL/SR-5100-60462; US Department of Energy, 2013; No. 1111191. DOI: 10.2172/1111191.
(51) Li, S.; Jiang, Y.; Snowden-Swan, L. J.; Askander, J. A.; Schmidt, A. J.; Billing, J. M. Techno-Economic Uncertainty Analysis of Wet Waste-to-Biocrude via Hydrothermal Liquefaction. *Appl. Energy* **2021**, *283*, No. 116340.
(52) Brown, T. R. A Techno-Economic Review of Thermochemical Cellulosic Biofuel Pathways. *Bioresour. Technol.* **2015**, *178*, 166−176.
(53) Paida, V. R.; Kersten, S. R. A.; Brilman, D. W. F. Hydrothermal Gasification of Sucrose. *Biomass Bioenergy* **2019**, *126*, 130−141.
(54) Wang, C.; Xie, T.; Kots, P. A.; Vance, B. C.; Yu, K.; Kumar, P.; Fu, J.; Liu, S.; Tsilomelekis, G.; Stach, E. A.; Zheng, W.; Vlachos, D. G. Polyethylene Hydrogenolysis at Mild Conditions over Ruthenium on Tungstated Zirconia. *JACS Au* **2021**, *1* (9), 1422−1434.
(55) Spiller, L. L. Determination of Ammonia/Air Diffusion Coefficient Using Nafion Lined Tube. *Anal. Lett.* **1989**, *22* (11−12), 2561−2573.
(56) Scheepers, D. M.; Tahir, A. J.; Brunner, C.; Guillen-Burrieza, E. Vacuum Membrane Distillation Multi-Component Numerical Model for Ammonia Recovery from Liquid Streams. *J. Membr. Sci.* **2020**, *614*, No. 118399.
(57) Ding, Z.; Liu, L.; Li, Z.; Ma, R.; Yang, Z. Experimental Study of Ammonia Removal from Water by Membrane Distillation (MD): The Comparison of Three Configurations. *J. Membr. Sci.* **2006**, *286* (1), 93−103.
(58) Al-Obaidani, S.; Curcio, E.; Macedonio, F.; Di Profio, G.; Al-Hinai, H.; Drioli, E. Potential of Membrane Distillation in Seawater Desalination: Thermal Efficiency, Sensitivity Study and Cost Estimation. *J. Membr. Sci.* **2008**, *323* (1), 85−98.
(59) Kogler, A.; Farmer, M.; Simon, J. A.; Tilmans, S.; Wells, G. F.; Tarpeh, W. A. Systematic Evaluation of Emerging Wastewater Nutrient Removal and Recovery Technologies to Inform Practice and Advance Resource Efficiency. *ACS EST Eng.* **2021**, *1* (4), 662−684.
(60) Seider, W. D.; Lewin, D. R.; Seader, J.D.; Widagdo, S.; Gani, R.; Ng, K. M. *Product and Process Design Principles: Synthesis, Analysis, and Evaluation*, 4th ed.; Wiley, 2016.
(61) Grady, C. P. L., Jr.; Daigger, G. T.; Love, N. G.; Filipe, C. D. M. *Biological Wastewater Treatment*, 3rd ed.; CRC Press: Boca Raton, 2011. DOI: 10.1201/b13775.
(62) Filipe, C. D. M.; Grady, C. P. L., Jr. *Biological Wastewater Treatment*, 2nd ed., Revised and Expanded; Taylor & Francis, 1998.
(63) Zhang, Z.; Li, W.; Zhang, G.; Xu, G. Impact of Pretreatment on Solid State Anaerobic Digestion of Yard Waste for Biogas Production. *World J. Microbiol. Biotechnol.* **2014**, *30* (2), 547−554.
(64) Lissens, G.; Klinke, H.; Verstraete, W.; Ahring, B.; Thomsen, A. B. Wet Oxidation Pre-Treatment of Woody Yard Waste: Parameter Optimization and Enzymatic Digestibility for Ethanol Production. *J. Chem. Technol. Biotechnol.* **2004**, *79* (8), 889−895.
(65) Malik, S. N.; Madhu, K.; Mhaisalkar, V. A.; Vaidya, A. N.; Mudliar, S. N. Pretreatment of Yard Waste Using Advanced Oxidation Processes for Enhanced Biogas Production. *Biomass Bioenergy* **2020**, *142*, No. 105780.
(66) Li, Y.; Zhang, X.; Morgan, V. L.; Lohman, H. A. C.; Rowles, L. S.; Mittal, S.; Kogler, A.; Cusick, R. D.; Tarpeh, W. A.; Guest, J. S. QSDsan: An Integrated Platform for Quantitative Sustainable Design of Sanitation and Resource Recovery Systems. *Environ. Sci. Water Res. Technol.* **2022**, *8* (10), 2289−2303.
(67) *Life Cycle and Cost Assessments of Nutrient Removal Technologies in Wastewater Treatment Plants*; United States Environmental Protection Agency, 2021.
(68) US EPA. About the Clean Water State Revolving Fund (CWSRF). *Clean Water State Revolving Fund*. https://www.epa.gov/cwsrf/about-clean-water-state-revolving-fund-cwsrf (accessed 2023-04-15).
(69) Swiss Centre for Life Cycle Inventories. *Ecoinvent 3.8 Database*. https://ecoinvent.org/the-ecoinvent-database/ (accessed 2023-01-06).
(70) Bare, J. TRACI 2.0: The Tool for the Reduction and Assessment of Chemical and Other Environmental Impacts 2.0. *Clean Technol. Environ. Policy* **2011**, *13* (5), 687−696.
(71) Li, Y.; Trimmer, J. T.; Hand, S.; Zhang, X.; Chambers, K. G.; Lohman, H. A. C.; Shi, R.; Byrne, D. M.; Cook, S. M.; Guest, J. S. Quantitative Sustainable Design (QSD) for the Prioritization of

Research, Development, and Deployment of Technologies: A Tutorial and Review. *Environ. Sci. Water Res. Technol.* **2022**, *8*, No. 2439.
(72) Slopiecka, K.; Liberti, F.; Massoli, S.; Bartocci, P.; Fantozzi, F. Chemical and Physical Characterization of Food Waste to Improve Its Use in Anaerobic Digestion Plants. *Energy Nexus* **2022**, *5*, No. 100049.
(73) Hao, B.; Xu, D.; Jiang, G.; Sabri, T. A.; Jing, Z.; Guo, Y. Chemical Reactions in the Hydrothermal Liquefaction of Biomass and in the Catalytic Hydrogenation Upgrading of Biocrude. *Green Chem.* **2021**, *23* (4), 1562−1583.
(74) Komilis, D. P.; Ham, R. K. The Effect of Lignin and Sugars to the Aerobic Decomposition of Solid Wastes. *Waste Manag.* **2003**, *23* (5), 419−423.
(75) Nynäs, A.-L.; Newson, W. R.; Johansson, E. Protein Fractionation of Green Leaves as an Underutilized Food Source—Protein Yield and the Effect of Process Parameters. *Foods* **2021**, *10* (11), 2533.
(76) Snowden-Swan, L. J.; Billing, J. M.; Thorson, M. R.; Schmidt, A. J.; Santosa, D. M.; Jones, S. B.; Hallen, R. T. *Wet Waste Hydrothermal Liquefaction and Biocrude Upgrading to Hydrocarbon Fuels: 2019 State of Technology*; PNNL-29882; Pacific Northwest National Lab. (PNNL): Richland, WA, United States, 2020. DOI: 10.2172/1617028.
(77) Snowden-Swan, L. J.; Billing, J. M.; Thorson, M. R.; Schmidt, A. J.; Jiang, Y.; Santosa, D. M.; Seiple, T. E.; Daniel, R. C.; Burns, C. A.; Li, S.; Hart, T. R.; Fox, S. P.; Olarte, M. V.; Kallupalayam Ramasamy, K.; Anderson, D. B.; Hallen, R. T.; Radovcich, S.; Mathias, P. M.; Taylor, M. A. *Wet Waste Hydrothermal Liquefaction and Biocrude Upgrading to Hydrocarbon Fuels: 2020 State of Technology*; PNNL-30982; Pacific Northwest National Lab. (PNNL): Richland, WA, United States, 2021. DOI: 10.2172/1771363.
(78) Snowden-Swan, L. J.; Li, S.; Jiang, Y.; Thorson, M. R.; Schmidt, A. J.; Seiple, T. E.; Billing, J. M.; Santosa, D. M.; Hart, T. R.; Fox, S. P.; Cronin, D.; Kallupalayam Ramasamy, K.; Anderson, D. B.; Hallen, R. T.; Fonoll-Almansa, X.; Norton, J. *Wet Waste Hydrothermal Liquefaction and Biocrude Upgrading to Hydrocarbon Fuels: 2021 State of Technology*; PNNL-32731; Pacific Northwest National Lab. (PNNL): Richland, WA, United States, 2022. DOI: 10.2172/1863608.
(79) Haider, M. S.; Castello, D.; Rosendahl, L. A. Two-Stage Catalytic Hydrotreatment of Highly Nitrogenous Biocrude from Continuous Hydrothermal Liquefaction: A Rational Design of the Stabilization Stage. *Biomass Bioenergy* **2020**, *139*, No. 105658.
(80) Martinez-Fernandez, J. S.; Chen, S. Sequential Hydrothermal Liquefaction Characterization and Nutrient Recovery Assessment. *Algal Res.* **2017**, *25*, 274−284.
(81) Hu, Y.; Feng, S.; Xu, C.; Bassi, A. Production of Low-Nitrogen Bio-Crude Oils from Microalgae Pre-Treated with Pre-Cooled NaOH/Urea Solution. *Fuel* **2017**, *206*, 300−306.
(82) Leng, L.; Zhang, W.; Peng, H.; Li, H.; Jiang, S.; Huang, H. Nitrogen in Bio-Oil Produced from Hydrothermal Liquefaction of Biomass: A Review. *Chem. Eng. J.* **2020**, *401*, No. 126030.
(83) Matayeva, A.; Rasmussen, S. R.; Biller, P. Distribution of Nutrients and Phosphorus Recovery in Hydrothermal Liquefaction of Waste Streams. *Biomass Bioenergy* **2022**, *156*, No. 106323.
(84) Liu, H.; Lyczko, N.; Nzihou, A.; Eskicioglu, C. Phosphorus Recovery from Municipal Sludge-Derived Hydrochar: Insights into Leaching Mechanisms and Hydroxyapatite Synthesis. *Water Res.* **2023**, *241*, No. 120138.
(85) Komilis, D.; Ham, R. K. *Life Cycle Inventory and Cost Model for Mixed Municipal and Yard Waste Composting*; United States Environmental Protection Agency, 2000.
(86) Li, Y.; Leow, S.; Dong, T.; Nagle, N. J.; Knoshaug, E. P.; Laurens, L. M. L.; Pienkos, P. T.; Guest, J. S.; Strathmann, T. J. Demonstration and Evaluation of Hybrid Microalgae Aqueous Conversion Systems for Biofuel Production. *ACS Sustain. Chem. Eng.* **2019**, *7* (6), 5835−5844.
(87) Ou, L.; Li, S.; Tao, L.; Phillips, S.; Hawkins, T.; Singh, A.; Snowden-Swan, L.; Cai, H. Techno-Economic Analysis and Life-Cycle Analysis of Renewable Diesel Fuels Produced with Waste Feedstocks. *ACS Sustain. Chem. Eng.* **2022**, *10* (1), 382−393.
(88) Zhao, Y.; Yang, Z.; Niu, J.; Du, Z.; Federica, C.; Zhu, Z.; Yang, K.; Li, Y.; Zhao, B.; Pedersen, T. H.; Liu, C.; Emmanuel, M. Systematical Analysis of Sludge Treatment and Disposal Technologies for Carbon Footprint Reduction. *J. Environ. Sci.* **2023**, *128*, 224−249.
(89) Yang, J.; He, Q.; Niu, H.; Corscadden, K.; Astatkie, T. Hydrothermal Liquefaction of Biomass Model Components for Product Yield Prediction and Reaction Pathways Exploration. *Appl. Energy* **2018**, *228*, 1618−1628.
(90) Baptista, A. I.; Perovich, A. *U.S. Municipal Solid Waste Incinerators: An Industry in Decline*; The Tishman Environment and Design Center, 2019.
(91) Lu, J.; Li, H.; Zhang, Y.; Liu, Z. Nitrogen Migration and Transformation during Hydrothermal Liquefaction of Livestock Manures. *ACS Sustain. Chem. Eng.* **2018**, *6* (10), 13570−13578.
(92) Badgett, A.; Newes, E.; Milbrandt, A. Economic Analysis of Wet Waste-to-Energy Resources in the United States. *Energy* **2019**, *176*, 224−234.
(93) PNNL Announces Hydrothermal Liquefaction Innovation. *Pacific Northwest National Laboratory*. https://www.pnnl.gov/publications/pnnl-announces-hydrothermal-liquefaction-innovation (accessed 2023-11-02).
(94) Liu, B.; Giannis, A.; Zhang, J.; Chang, V. W.-C.; Wang, J.-Y. Characterization of Induced Struvite Formation from Source-Separated Urine Using Seawater and Brine as Magnesium Sources. *Chemosphere* **2013**, *93* (11), 2738−2747.
(95) Thyberg, K. L.; Tonjes, D. J.; Gurevitch, J. Quantification of Food Waste Disposal in the United States: A Meta-Analysis. *Environ. Sci. Technol.* **2015**, *49* (24), 13946−13953.
(96) Vardon, D. R.; Sharma, B. K.; Scott, J.; Yu, G.; Wang, Z.; Schideman, L.; Zhang, Y.; Strathmann, T. J. Chemical Properties of Biocrude Oil from the Hydrothermal Liquefaction of Spirulina Algae, Swine Manure, and Digested Anaerobic Sludge. *Bioresour. Technol.* **2011**, *102* (17), 8295−8303.
(97) Sharma, N.; Jaiswal, K. K.; Kumar, V.; Vlaskin, M. S.; Nanda, M.; Rautela, I.; Tomar, M. S.; Ahmad, W. Effect of Catalyst and Temperature on the Quality and Productivity of HTL Bio-Oil from Microalgae: A Review. *Renew. Energy* **2021**, *174*, 810−822.
(98) Subramaniam, S.; Santosa, D. M.; Brady, C.; Swita, M.; Ramasamy, K. K.; Thorson, M. R. Extended Catalyst Lifetime Testing for HTL Biocrude Hydrotreating to Produce Fuel Blendstocks from Wet Wastes. *ACS Sustain. Chem. Eng.* **2021**, *9* (38), 12825−12832.
(99) Thorson, M. R.; Santosa, D. M.; Hallen, R. T.; Kutnyakov, I.; Olarte, M. V.; Flake, M.; Neuenschwander, G.; Middleton-Smith, L.; Zacher, A. H.; Hart, T. R.; Schmidt, A. J.; Lemmon, T.; Swita, M. Scaleable Hydrotreating of HTL Biocrude to Produce Fuel Blendstocks. *Energy Fuels* **2021**, *35* (14), 11346−11352.
(100) Biller, P.; Sharma, B. K.; Kunwar, B.; Ross, A. B. Hydroprocessing of Bio-Crude from Continuous Hydrothermal Liquefaction of Microalgae. *Fuel* **2015**, *159*, 197−205.
(101) Collin, T. D.; Cunningham, R.; Asghar, M. Q.; Villa, R.; MacAdam, J.; Jefferson, B. Assessing the Potential of Enhanced Primary Clarification to Manage Fats, Oils and Grease (FOG) at Wastewater Treatment Works. *Sci. Total Environ.* **2020**, *728*, No. 138415.
(102) Li, Y.; Strathmann, T. J. Kinetics and Mechanism for Hydrothermal Conversion of Polyhydroxybutyrate (PHB) for Wastewater Valorization. *Green Chem.* **2019**, *21* (20), 5586−5597.
(103) Hu, S.; Luo, X.; Li, Y. Polyols and Polyurethanes from the Liquefaction of Lignocellulosic Biomass. *ChemSusChem* **2014**, *7* (1), 66−72.
(104) Liu, H.; Lyczko, N.; Nzihou, A.; Eskicioglu, C. Phosphorus Extracted Municipal Sludge-Derived Hydrochar as a Potential Solid Fuel: Effects of Acidic Leaching and Combustion Mechanism. *Chem. Eng. J.* **2023**, *473*, No. 145191.
(105) Abeyratne, W. M. L. K.; Abeysiriwardana-Arachchige, I. S. A.; Bayat, H.; Zhang, Y.; Brewer, C. E.; Nirmalakhandan, N. Feasibility of

Hydrothermal Liquefaction in Phosphorus-Recovery from Wastewater Sludges. *J. Water Process Eng.* **2023**, *55*, No. 104174.
(106) Swetha, A.; ShriVigneshwar, S.; Gopinath, K. P.; Sivaramakrishnan, R.; Shanmuganathan, R.; Arun, J. Review on Hydrothermal Liquefaction Aqueous Phase as a Valuable Resource for Biofuels, Bio-Hydrogen and Valuable Bio-Chemicals Recovery. *Chemosphere* **2021**, *283*, No. 131248.

https://doi.org/10.1021/acs.est.3c07394
Environ. Sci. Technol. 2024, 58, 2528−2541